Published in final edited form as:
Opt Lett. 2012 March 1; 37(5): 812–814.

Label-free 3D imaging of microstructure, blood and lymphatic vessels within tissue beds *in vivo*

Zhongwei Zhi, **Yeongri Jung**, and **Ruikang K. Wang***
Department of Bioengineering, University of Washington, Seattle, WA 98195, USA

Abstract

This letter reports the use of an ultrahigh resolution optical microangiography (OMAG) system for simultaneous 3D imaging of microstructure, lymphatic and blood vessels without the use of exogenous contrast agent. An automatic algorithm is developed to segment the lymphatic vessels from the microstructural images, based on the fact that the lymph fluid is optically transparent. The OMAG system is developed that utilizes a broadband supercontinuum light source, providing an axial resolution of 2.3 μm and lateral resolution of 5.8 μm, capable of resolving the capillary vasculature and lymphatic vessels innervating microcirculatory tissue beds. Experimental demonstration is performed by showing detailed 3D lymphatic and blood vessel maps, coupled with morphology, within mouse ears *in vivo*.

Lymphatic system is responsible for immune function and waste drainage. Clinical and pathological observations suggest that, transport of tumor cells via lymphatics is the most common pathway of initial dissemination for many carcinomas. Visualization of the lymphatic system (lymph nodes and lymphatic vessels) plays a significant role in assessing patients with various malignancies and lymphedema [1, 2]. Most current methods for visualizing the lymphatic vessels require exogenous contrast agents [3], including but not limited to Evans blue dye imaging, fluorescence imaging, MRI, CT, Ultrasound and Photoacoustic imaging (Indocyanine Green dye as contrast agent) [4]. Unfortunately, the applicability of these methods is limited due to the difficulty of contrast agent uptake and their potential side effects. There is a need for a noninvasive and label-free method that can image the lymphatic vessel network *in vivo*.

Due to the relative low scattering property of lymph fluid, it appears almost transparent optically. In this regard, an endogenous contrast would be taken advantage by optical coherence tomography (OCT) [5], which is an interferometric technology using the intrinsic light scattering as image contrast. This was initially demonstrated by B. J. Vakoc et al. [6] using the negligible OCT scattering intensity from the lymph fluid to delineate lymph vessels, which was correlated with Evan's blue dye image. Our previous work that used label-free optical microangiography (OMAG), a variation of OCT technology) reported the 3D information of microcirculation that supplies the lymph node and efferent lymph vessels [7]. However, both of these works was unable to show lymphatic capillaries due to their limited spatial resolution. In order to distinguish the lymphatic vessel, especially the lymphatic capillaries from background tissue, ultrahigh resolution is required. Another issue we wish to address is that to better understand the physiological function of the immune system, it is preferred to study the interaction between lymphatic circulation system and blood microcirculation. This requires high resolution imaging of microstructure, lymphatic

*Corresponding author: wangrk@uw.edu.

and blood vessel network within tissue bed all together. In this letter we report the use of an ultrahigh resolution OMAG system for simultaneous 3D imaging of microstructure, blood vessels and lymphatic vessels innervating the living perfused tissue beds without the use of any contrast agents.

The OMAG system setup used here is similar to that previously reported [8]. Briefly, the system utilized a broadband supercontinuum light source as the illumination light, which provided a bandwidth of 120 nm centered on 800 nm, delivering an axial resolution of 2.3 μm in tissue. The objective lens with an effective focal length of 18 mm provides a measured lateral resolution of 5.8 μm. With the 2.3 μm axial and 5.8 μm lateral resolutions, we were able to image blood vessel and lymph vessel down to the capillary level within microcirculatory tissue beds. The high speed spectrometer that was used to capture the OCT interferograms employed a high speed CMOS line-scan camera with 4096 active pixel array (Basler SPL 4096-70 KM, Germany), capable of a maximum line scan rate at 70 kHz. The system had a measured sensitivity of 95 dB at the 0.5 mm depth position, dropped to 87 dB at 1.5 mm with 4.0 mw power incident on the sample.

In order to perform simultaneous 3D imaging of blood and lymphatic vessels, we applied the OMAG scanning protocol reported in [9] for this study. A 3D data volume with 256 A-lines and 1024 B-frames (256 cross-sections with 4 B-frames at each cross-section) was captured to cover a field of view of 1.2×1.2 mm^2. With the camera running at 70 kHz line scan rate, it provided an image acquisition rate of 220 frames per second. Under this configuration, the whole 3D dataset was acquired within 5 seconds, which minimized the possible motion artifact.

By processing the data using the OMAG algorithm [8], we were able to simultaneously obtain two images: microstructure and blood flow images. The microstructure image at each cross-section was obtained by averaging four images captured at the same cross-section, which reduced the random noise and made the microstructure image smooth. Finally, the lymphatic vessel image was extracted from the microstructure image.

We developed an automatic segmentation algorithm for the extraction of lymphatic vessel from the OCT microstructure image, based on the fact that the lymph fluid is optically transparent, thus giving optical signals near the system noise floor. The segmentation program was developed on OpenCV environment, which is an image processing library. In the program, an adaptive threshold was first calculated by the intensity of the pixels within a local window around a target pixel to perform binarization operation. The window size was designed to be adjustable according to local lymphatic vessel size. If the intensity of target pixel was lower than the adaptive threshold, then that target pixel was judged to belong to lymphatic vessel, and assigned to a value of 1; otherwise it was assigned to 0. Finally, the processing was performed frame by frame for the whole 3D dataset to obtain a final 3D data volume, showing the lymphatic vessels only. Compared to the method that used only one fixed threshold to perform binarization for the whole image, the use of the adaptive threshold can extract the target tissue at where the intensities of both target tissue and surrounding tissue are either high or low.

To demonstrate the capability of our ultra-high resolution OAMG system and proposed segmentation method for simultaneous imaging of blood vessel and lymphatic vessel, we conducted experiments to image the microstructure, blood vessel and lymphatic vessel networks lying within the mouse ear pinna in vivo. C57 BL/6 mice (22 to 26 g) were immobilized in a stereotaxic stage and anesthetized with vaporized isoflurane (0.2 L/min oxygen and 0.8 L/min air). The body temperature was kept to 35.5 and 36.5 °C with use of a heat pad. The ear pinna was hair-removed and placed flatten for imaging. All experimental

animal procedures performed in this study conform to the guidelines of the US National Institutes of Health. The laboratory animal protocol was approved by the Animal Care and Use Committee of University of Washington.

Fig.1 shows results of depth-resolved lymphatic vessels from living mouse ear tissue. Fig.1 (b) illustrates one typical cross-sectional microstructure image that slices through lymphatic vessels, the lumen of which gives the low optical scattering signals (appearing black in the image) due to the optical transparency of the flowing lymph fluid. Fig.1 (a) plots the signal intensity over the depth along the red line marked in (b), demonstrating there is almost no optical signal measured from the lumen of lymphatic vessel. Since the OMAG/OCT is depth-resolved imaging tool, the captured 3D dataset can be manipulated to show detailed microstructure information in any orientations. Fig.1 (c) and (d) are two en-face images that were extracted at the depth positions of 80 and 40 μm respectively, showing different lymphatic vessel patterns. With the proposed segmentation algorithm applied, 3D lymphatic vessel network within the scanned tissue volume can be obtained (Fig.1 (e)), which can be merged with the 3D microstructural image to show in detail how the lymphatic vessels are distributed within the tissue beds (Fig.1 (f)).

Most importantly, the spatial resolution afforded by our current imaging system enables the visualization of the one-way valve of lymphatic vessels, which prevent any backward flow. The sernilunar shaped lymphatic valve is marked by a blue circle in fig.1 (b) and pointed by arrows in fig 1 (d) and (e) as well.

Fig.2 demonstrates the capability of the proposed system and segmentation method for simultaneous 3D vascular-angiography and lymphangiography where fig.2 (a) and (b) show blood vessel image and lymphatic vessel image, respectively, obtained from the same tissue volume. One advantage of the OMAG modality is that it is capable of providing co-registered and depth-resolved blood flow and lymphatic flow images in parallel. Thus, we merged the lymphatic vessels together with the blood vessels [fig.2 (c)] to better appreciate their positional relationship. Together with Fig.1, we noticed that lymphatic capillaries are closed at one end, which appearance is different from blood capillaries that are usually connected at both ends. According to the standard physiology textbook, this is due to that the function of lymphatic capillary is to drain excess tissue fluids within the extracellular space that must flow in one direction only. Fig.2 (d) shows a maximum intensity projection view of blood vessels lying on the merged microstructure and lymphatic vessel image. Analyses of morphological features of blood vessels, lymphatic vessels and microstructures of the microcirculation tissue beds in vivo afforded by the 3D OMAG dataset provides detailed information about blood flow in both lymphatic tissue volumes and individual circulation vessels. OMAG thus may be a useful tool for the investigations of potential mechanisms of the normal physiological functions as to lymph and blood perfusions, as well as their responses to the therapeutic treatment under diseased conditions, e.g., inflammation and cancer. Previous methods, such as Intravital Microscopy [10] and Multiphoton Microscopy [11], have been limited to small field of view and superficial depths (<200 μm), and often required labeling contrast agents to reveal the lymph vessels. OMAG is superior in visualizing complex morphological features, blood and lymph vessel networks deeper (>200 μm) and without the use of the contrast agents.

Fig.3 shows a wide projection view of the detailed (a) blood vessel and (b) lymphatic vessel network within a scanned microcirculatory tissue beds covering $4 \times 4 mm^2$ of the mouse ear. Both dense blood capillary and lymph capillary could be visualized and correlated with each other. Without the need for exogenous contrast agents, OMAG thus have potential to monitor functional lymphatic and blood vessels within the tissue beds in vivo both locally and globally. Notably, the OMAG lymphangiography can be performed simultaneously with

the tissue morphology and vascular microangiography; and these can be done from one single OMAG volumetric scan.

In conclusion, we have demonstrated that ultrahigh resolution OAMG is able to achieve simultaneous 3D label-free lymphangiography and vascular-angiography coupled with detailed tissue morphology in vivo. We have also demonstrated that the high resolution afforded by OMAG enables the visualization of the lymphatic valve structure, promising future investigation of the lymph flow dynamics within deep microcirculatory tissue beds that has not been possible previously. In future, the quantitative measurement of lymphatic vessel density will also be useful for the evaluation of lymphangiogenesis, which may be associated with the occurrence of various diseases especially tumor metastasis.

Acknowledgments

The authors would like to thank Dr. Xin Yin for his help. This work was supported in part by National Institutes of Health (NIH) grants R01 HL093140, R01 EB009682, and R01 DC010201, and the American Heart Association (0855733G).

Detailed References

1. Alitalo K, Tammela T, Petrova TV. Lymphangiogenesis in development and human disease. Nature. 2005; 438:946–953. [PubMed: 16355212]
2. Pepper MS. Lymphangiogenesis and tumor metastasis: Myth or reality? Clinical Cancer Research. 2001; 7:462–468. [PubMed: 11297234]
3. Zhang F, Niu G, Lu GM, Chen XY. Preclinical Lymphatic Imaging. Molecular Imaging and Biology. 2011; 13:599–612. [PubMed: 20862613]
4. Kim C, Song KH, Gao F, Wang LHV. Sentinel Lymph Nodes and Lymphatic Vessels: Noninvasive Dual-Modality in Vivo Mapping by Using Indocyanine Green in Rats-Volumetric Spectroscopic Photoacoustic Imaging and Planar Fluorescence Imaging. Radiology. 2010; 255:442–450. [PubMed: 20413757]
5. Huang D, Swanson EA, Lin CP, Schuman JS, Stinson WG, Chang W, Hee MR, Flotte T, Gregory K, Puliafito CA, et al. Optical coherence tomography. Science. 1991; 254:1178–1181. [PubMed: 1957169]
6. Vakoc BJ, Lanning RM, Tyrrell JA, Padera TP, Bartlett LA, Stylianopoulos T, Munn LL, Tearney GJ, Fukumura D, Bouma BE. Three-dimensional microscopy of the tumor microenvironment in vivo using optical frequency domain imaging. Nature Medicine. 2009; 15:1219–U1151.
7. Jung Y, Zhi Z, Wang RK. Three-dimensional optical imaging of microvascular networks within intact lymph node in vivo. J Biomed Opt. 2010; 15:050501. [PubMed: 21054073]
8. Zhi ZW, Qin J, An L, Wang RK. Supercontinuum light source enables in vivo optical microangiography of capillary vessels within tissue beds. Optics Letters. 2011; 36:3169–3171. [PubMed: 21847196]
9. Zhi Z, Jung Y, Jia Y, An L, Wang RK. Highly sensitive imaging of renal microcirculation in vivo using ultrahigh sensitive optical microangiography. Biomed Opt Express. 2011; 2:1059–1068. [PubMed: 21559119]
10. Galanzha EI, Tuchin VV, Zharov VP. In vivo integrated flow image cytometry and lymph/blood vessels dynamic microscopy. J Biomed Opt. 2005; 10:054018. [PubMed: 16292978]
11. Miller MJ, Wei SH, Parker I, Cahalan MD. Two-photon imaging of lymphocyte motility and antigen response in intact lymph node. Science. 2002; 296:1869–1873. [PubMed: 12016203]

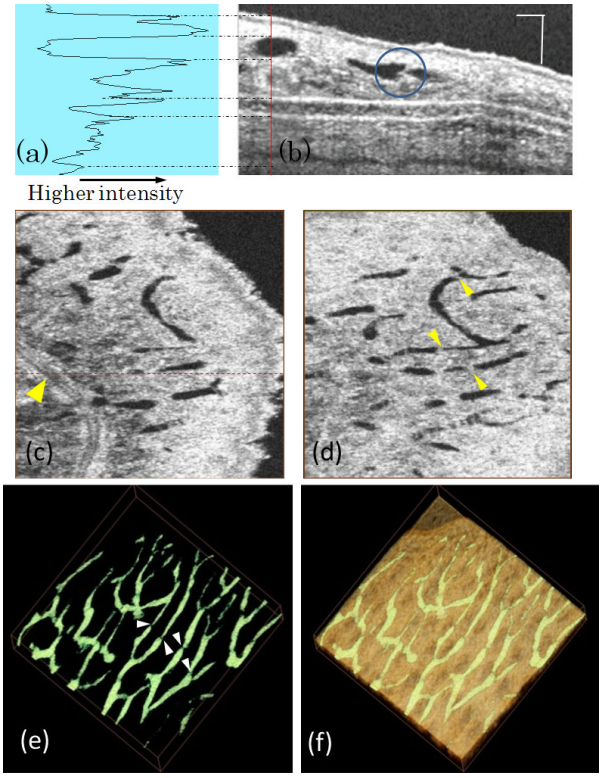

Fig. 1.

Ultra-high resolution OCT image based lymphangiography. (a) Plot of signal intensity along the red line in, (b) one typical cross-sectional microstructure image of mouse ear; (c) en-face image of mouse ear at the depth of 40 μm, where the red dashed line indicates the cross-section in (b) and yellow arrow points to a blood vessel; (d) en-face image at the depth of 80 μm; (e) 3D lymphatic vessel network and (f) 3D merge of lymphatic vessel with the microstructure image. Scale bar= 100 μm and image size for (c)-(f) is 1.2 × 1.2 mm^2.

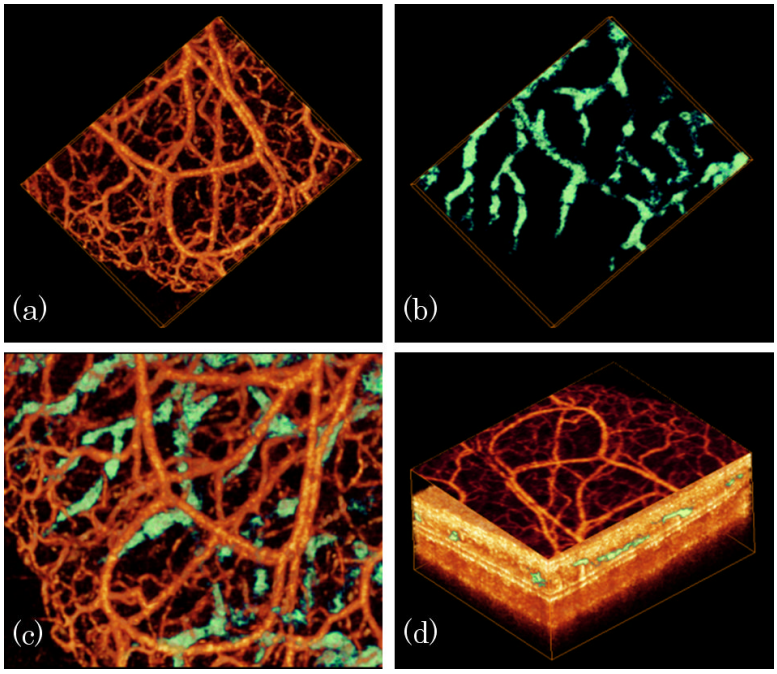

Fig. 2.
In vivo simultaneous 3D angiography and lymphangiography of mouse ear pinna. (a) Blood vessel image, (b) lymphatic vessel, (c) combined blood and lymphatic vessel image and (d) projection view of blood vessel lying on merged microstructure and lymphatic vessel image.

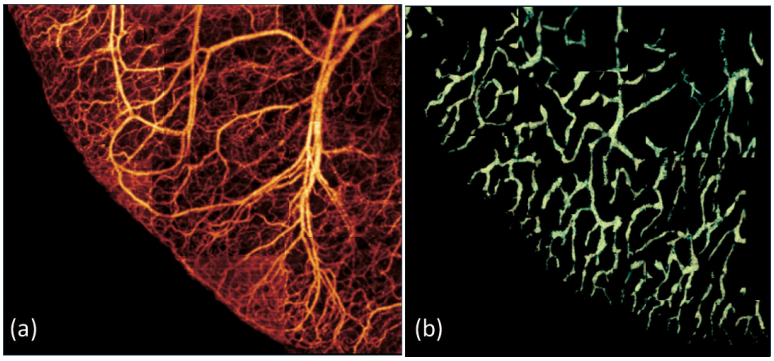

Fig. 3.
Wide field ($4 \times 4mm^2$) projection view of (a) blood vessel map and (b) lymphatic vessel network captured within the same tissue beds merged by multiple images.